



## Structural and Optical Properties for ZnO Nanoparticles for Antibacterial Application

Aso Abdullah Saeed 

Department of Electrical Technique, Sulaimani Technical Institute, Sulaimani polytechnic University, Iraq

Received: 25 Sep. 2024 Received in revised form: 7 Dec. 2024 Accepted: 19 Dec. 2024

Final Proofreading: 2 Jan. 2025 Available online: 25 Feb. 2025

### ABSTRACT

In this research, ZnO nanoparticles were prepared by pulsed laser ablation in liquid (PLAL) technique. The X-Ray diffraction (XRD) test was used to find out the crystal structure of ZnO and its crystal size, the result is that the creation of ZnO NPs has a polycrystalline structure of hexagonal phases. As for an atomic force microscopy (AFM) analysis, AFM 3D pictures show that the surface roughness are increase with increase the laser energy. The UV-visible device test was conducted to determine the optical properties, and it was revealed that the maximum absorption appears to occur at (400 nm). By changing the laser energy discovered that when laser intensity increased, the ZnO NPs' bandgap decreases. ZnO has been used in antibacterial applications, The result of laser manufactured ZnO Nanoparticles was verified for its antibacterial activities at gram- positive (*Staphylococcus aureus*).

**Keywords:** Zinc oxide nanoparticles, PLAL, XRD, AFM, Antibacterial applications.

**Name:** Aso Abdullah Saeed

**E-mail:** [aso.abdullah@spu.edu.iq](mailto:aso.abdullah@spu.edu.iq)



©2025 THIS IS AN OPEN ACCESS ARTICLE UNDER THE CC BY LICENSE  
<http://creativecommons.org/licenses/by/4.0/>

## الخصائص البنيوية والبصرية لجسيمات أكسيد الزنك النانوية واستخدامه في التطبيقات المضادة

### للبكتيريا

اسو عبد الله سعيد

قسم تقنيات الكهريائية، معهد السلیمانیه التقنی، جامعة السلیمانیه التقنیة، السلیمانیه، العراق

### الملخص

في هذه الدراسة، تم تصنيع جسيمات أكسيد الزنك النانوية باستخدام تقنية الاستئصال بالليزر النبضي في السائل (PLAL). تم استخدام اختبار حيود الأشعة السينية (XRD) لمعرفة التركيب البلوري لأكسيد الزنك وحجمه البلوري، والنتيجة هي تكوين أكسيد الزنك النانوية متعدد التبلور هيكل المراحل السداسية. أما بالنسبة للتحليل المجهرى للقوة الذرية (AFM)، تظهر صورة الثلاثي الابعاد لـ AFM أن خشونة السطح يزداد بزيادة طاقة الليزر. تم إجراء اختبار الجهاز المرئي فوق البنفسجي لتحديد الخواص البصرية، وتبين أن الحد الأقصى للامتصاص يبدو أنه يحدث عند (400 nm). تم اكتشاف أنه عندما زادت شدة الليزر، تقلصت فجوة نطاق أكسيد الزنك النانوية. تم استخدام أكسيد الزنك في التطبيقات المضادة للبكتيريا، وتم التحقق من نتيجة بأن جزيئات أكسيد الزنك النانوية المصنعة بالليزر لنشاطها المضاد للبكتيريا عند إيجابية الجرام (المكورات العنقودية الذهبية).

### 1. INTRODUCTION

Nanomaterials are that distinct class of advanced materials that can be produced with the size of their internal dimensions or grains ranging from (1 - 100 nm) <sup>(1)</sup>. The phase of great development of nanomaterials preparation methods has led to various studies of these and the preparation at high-purity requirements and nanomaterials homogeneous thicknesses requiring high-cost precise systems and devices, all of which led to the search for a solution to this problem using less costly preparation methods and less complex devices. The laser ablation method to producing of nanoparticles used more inexpensive, less complex devices, has a high heat capacity and safe <sup>(2)</sup>. The properties of nanomaterials are radically different from the properties of bulk materials in terms of electrical conductivity, color, strength, and weight changes; beside that, the ratio of surface atoms to volume in nanomaterials is higher compared to bulk materials<sup>(3)</sup>. The comparatively large excitement binding energy (60 meV) comparison to thermal energy (26 meV). This semiconductor is

commonly referred to as II–VI, due to the fact that Zinc is part of the II group, and Oxygen belongs to the VI group on the periodic table. It boasts rising transmittance in the visible light zone. ZnO possesses several attractive features, including great electron mobility, not toxic, adaptable refractive index, and easy coating through anisotropic growth <sup>(4)</sup>. The energy level of the laser that is used to produce ZnO nanoparticles proportionally affects on the particle size, and that leads to decreasing the energy gap when the particle size reduces <sup>(5)</sup>.

Crystal structure of zinc oxide: There are three systems of zinc oxide crystals, the hexagonal wurtzite structure is a commonly observed crystal structure, along with the cubic zinc blend. The cubic rock salt structure, on the other hand, is rarely observed. The wurtzite structure is highly stable in its surrounding conditions. However, the zinc blend shape can be steadied through growing ZnO on substrates to cubic lattice structure. Zn and oxygen form tetrahedral centers in different ways.

Various techniques have been used to produce different structures of zinc oxide nanoparticles, each with unique characteristics that make them appropriate for a wide variety of applications. These nanomaterials include nanowires, nanotubes, nanorods, nanoparticles, nanoclusters, and nanocrystals<sup>(6)</sup>. The ZnO nanoparticles are semi-spherical form of hexagonal wurtzite, and clear distribution of size, and crystalline size that obtained by using Debye Scherrer's formula of XRD pattern method increase when increase energy level of laser<sup>(7)</sup>. Also, the surface smoothing of the ZnO nanoparticles is relative with the spherical shape of nanoparticles that can be shown by AFM<sup>(8)</sup>. The roughness changes with varies of different laser energies<sup>(9)</sup>. The ZnO nanoparticles utilize in widely range used in biological and environmental applications such as antibacterial, protein kinase inhibition, antidiabetic activity, antioxidant and some other fields<sup>(10,11)</sup>.

The aim of research is to study the changing structure and optical properties of ZnO nanoparticles when change the energy level of laser that used to obtain the nanoparticles and its effect when used as antibacterial.

## 2. EXPERIMENTAL PART

In order to create Zinc oxide nanoparticles, a piece of high-purity Zn metal (99.99 %) was placed in a glass pot with (2 ml) of distilled water. The glass vessel was exposed to a nanosecond pulsed ND: YAG laser with a wavelength of (1064 nm). To maintain consistent irradiation on the target and enhance the diffusion of particles, the glass vessel was rotated using a stepper motor at (6 rpm). This ensured a steady movement of distilled water. The distance between the Zinc (target) and the laser lens is (10 cm), the number of pulses is (1000 pulse) and repetition rate (5 Hz). The colloidal solution was obtained with a light yellow color after resection to create a thin film, the quartz slides are positioned on a hot lamina at a temperature of (90 °C). The drop-casting method of the colloidal solution as the [Figure \(1\)](#). We

obtain several samples with different laser fluency from (500, 600 and 700 J/cm<sup>2</sup>).

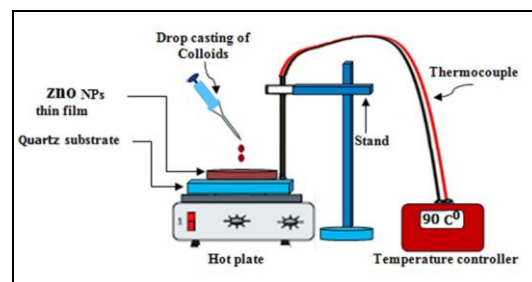


Fig. 1: The drop - casting technique<sup>(12)</sup>.

## 3. RESULTS

### 3.1. X-ray diffraction (XRD)

The X-ray diffraction patterns were measured for the Zinc Oxid NPs powder exposing to Nd -YAG lasers. Altogether the patterns were measured in the zone of (30–90 (2θ)) as shows in the [Figure \(2, 3, and 4\)](#) which shows that formation ZnO NPs has a polycrystalline structure and the hexagonal stage for ZnO NPs that agree with (JCPDS number: 89-1397). The peaks were at plane (100), (002), (101), (012), (110), and (013)<sup>(13)</sup>, and close agreement in (100), (002) and (101) in laser power (500, 700) with result of<sup>(14)</sup>.

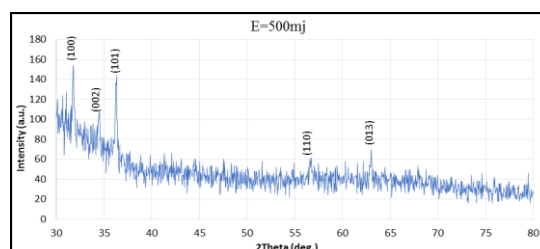


Fig. 2: The XRD pattern of Zinc Oxid NPs with laser energy 500 mJ.

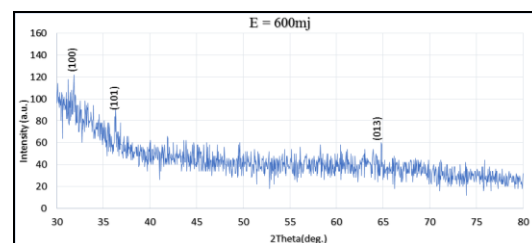
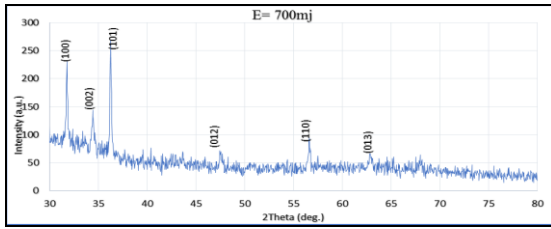


Fig. 3: The XRD pattern of Zinc Oxid NPs with laser energy 600 mJ.



**Fig. 4:** The XRD pattern of Zinc Oxid NPs with laser energy 700 mJ.

The diffraction patterns indicate sharp peaks, which suggest good crystallinity of the nano powders. A pattern was prepared at different laser energy levels (500, 600, and 700 mJ), and the samples showed diffraction peaks of Zinc Oxide that properly matched the hexagonal wurtzite structure. The broadened XRD patterns suggest an increase in the size of the manufactured ZnO NPs. The crystalline size is measured by using Debye-Scherrer formula:

$$D = K \lambda / \beta \cos \theta \quad \dots(1)$$

Where: D is size of nanoparticles, K is the shape coefficient for the reciprocal lattice point about 0.94 for spherical crystallites,  $\lambda$  is the wavelength of the X-ray source used (0.15418 nm for Cu k-alpha),  $\beta$  is the full width at half maximum and  $\theta$  is

the angle of diffraction. [Table \(1\)](#) shows an improvement in the creation of ZnO crystalline, and the crystalline size is measured in [Table \(1\)](#).

**Table 1:** crystallite size of Zinc oxide NPs prepared at different laser energies.

Energy (m J)	Crystallite size (nm)
500	35
600	44
700	62

### 3.2. Atomic force microscope (AFM)

[Figure \(5\)](#) displays an AFM image of ZnO NPs obtained through various laser energy levels (500, 600, and 700 m J). The results indicate that as the laser power increases, the particle size decreases. This behavior is evident from the figures where the morphology and size of ZnO NPs vary with increasing laser energy. Also the increasing energy level of laser leads to increase of average roughness of the nanoparticles which agree with<sup>(15)</sup>. The mean diameter of ZnO NPs prepared under changed energy with Root mean square values and its mean roughness of surface are listed in [Table \(2\)](#).

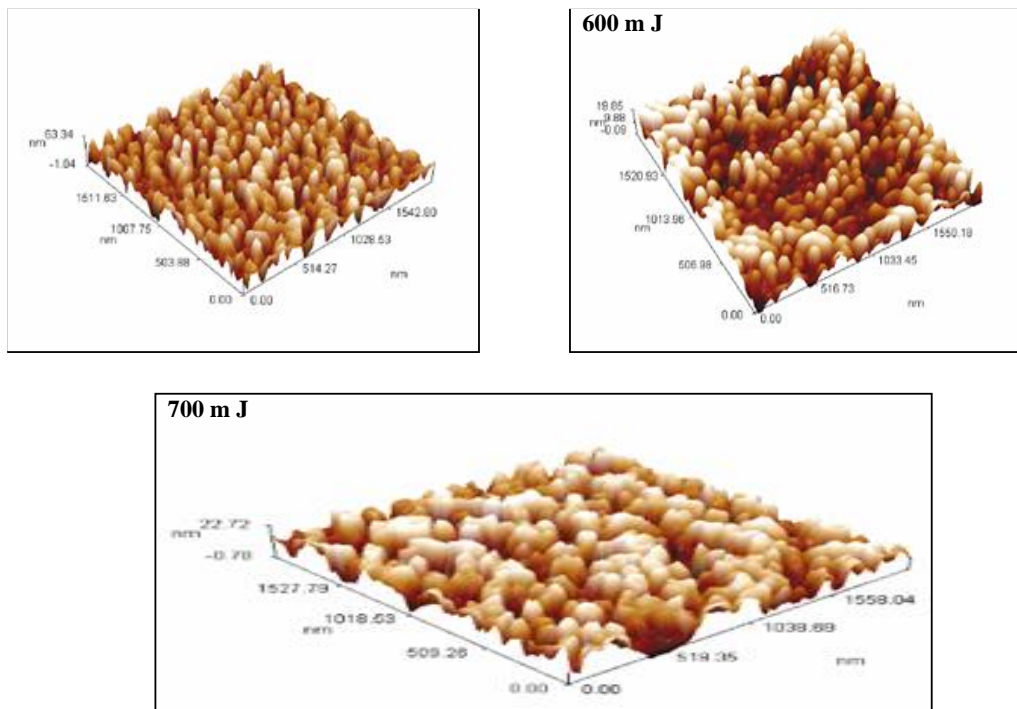


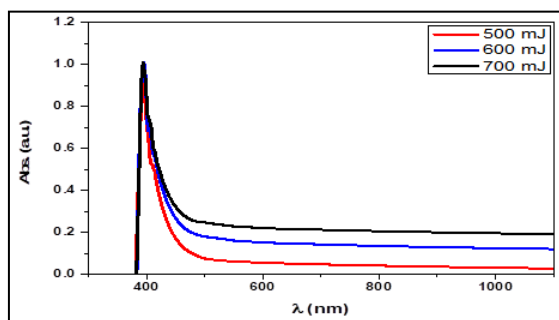
**Fig. 5:** 3D AFM pictures of Znic oxide NPs prepared at different laser energies.

**Table 2: The mean diameter and roughness of Zinc Oxide NPs prepared below different laser energies.**

Energy (mJ)	Mean grain size (nm)	Root mean Sq. (nm)	Mean Roughness (nm)
500	70.03	14	5.43
600	81.60	5.5	4.74
700	87.65	6.34	11.6

### 3.3. Optical properties

Figure (6) display the absorbance spectra of Zinc Oxide NPs, which are different with changed laser energy (500, 600, and 700 mJ), where the figure displays the absorption as a function of wavelength. It is exposed that super absorption seems to below (400 nm). As the laser energy rise, more particles are removed from the surface of the target, the concentration of NPs increased, causing a rise in the absorption spectrum for certain crops. This increase in intensity led to a corresponding rise in the Plasmon peak, which was further amplified by an increase in laser energy. The NP concentration has increased, as shown by the rise in spectra. The spectra display Plasmon resonance peaks of zinc oxide because of quantum size effects, that agree with <sup>(12)</sup>. The plasmon resonance appears as a result of our use of zinc as a metal.

**Fig. 6: The absorption spectrum of ZnO at different energies.**

The absorption spectra is used to illustrate the energy bandgap of ZnO Nanoparticle. Figure (7) shows a chart of  $(\alpha h\nu)^2$  with varying energy. The

Table (3) displays the energy bandgap of ZnO Nanoparticle, which decreases started to be (3.4 eV) and lessening to (2.8 eV) with a reduction in particle size. This reduction in particle size resulted in a change in the band structure and material properties. On the contrary, an increase in NP size leads to a decrease in bandgap. Larger energy systems show that the transmission bands of s-electrons and p-electrons are not bound from each other, allowing for an overlay incidence in circumstances with fewer particles. In a Fermi level range, the nuclear potential for the conduction of electrons is minimal, making each transition with permitted quantum numbers possess an absorption energy similar to conduction band energy. This may lead to a rise of defective states, leading to an increase in the absorption coefficient. Photon absorption produces electron-hole pairs, and the arena produced by such pairs could change the electronic structure and optical Nanomaterial characteristics. This is in agreement with <sup>(16)</sup>.

The energy gap of all models can be calculated at different the laser energy (500, 600 and 700 m J), as shown in the Table (3) and Figure (7) by the calculation

$$\alpha h\nu = B (h\nu - E_g)^{1/n} \quad \dots (2)$$

(B) transition static is equal to (1)· ( $\alpha$ ) absorption coefficient, (n) equal (1/2) at allowed direct transition and (n) equal (3/2) at forbidden direct transition.

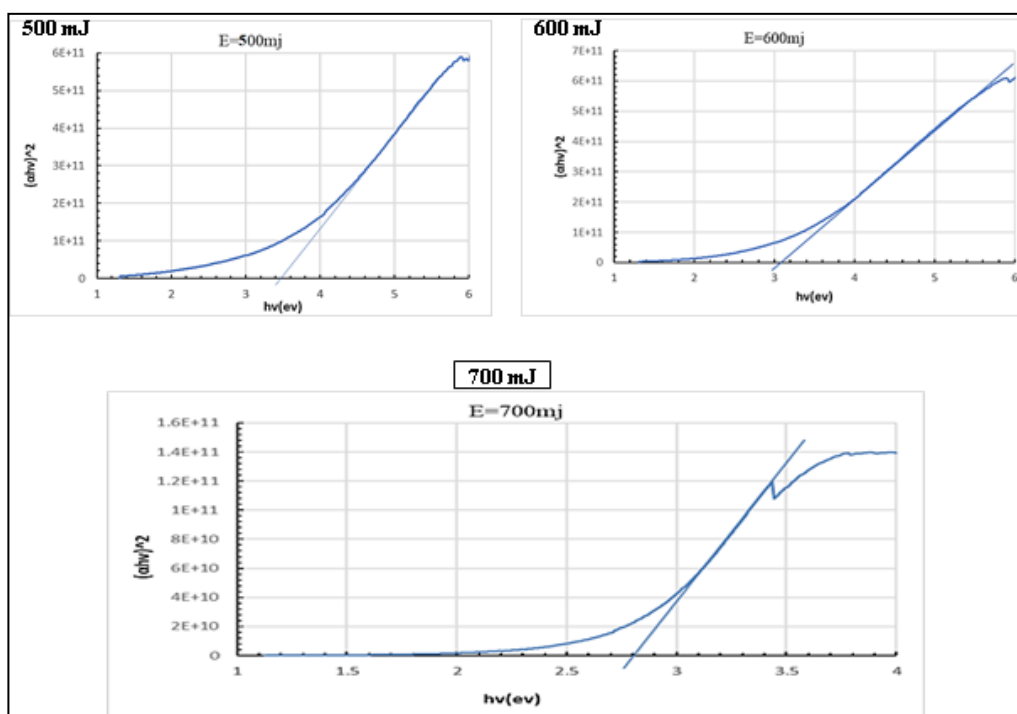


Fig. 7: The energy gap of Zinc Oxide Nps at different laser energies.

Table 3: The energygap of Zinc Oxide NPs prepared under different laser energies.

Laser energy (mJ)	Energy gap (eV)
500	3.4
600	3.1
700	2.8

### 3.4. Antibacterial measurements

The result of the laser synthesized ZnO nanoparticles were tested at own antibacterial doings across gram positive (*Staphylococcus aureus*). The one of mechanism of ZnO Nanoparticles effect on the bacterial that the cell membrane lipids and proteins of gram-positive bacteria is made up of a peptidoglycan molecule and is notably thick. Due to the positively charged nature of  $Zn^{+2}$  ions and the negative charge of peptidoglycan, there is an electrostatic attraction

between these positive and negative ions that resulted in the leakage of intracellular contents and eventually the death of cells (17, 18).

Antibacterial activities were evaluated, as [Figure \(8\)](#) And [Table \(4\)](#). ZnO appear to effect on it. From the figure, the ZnO nanoparticles obtained from the experiment demonstrated significant effectiveness against bacterial strains, particularly Gram-positive bacteria. Our findings were compared to previous research and it was discovered that the new ZnO had exceptional efficacy, which is consistent with the results of (19, 20).

We note from the results of the [Table \(4\)](#) that increasing the laser energy from (500, 600 and 700 mJ) for ZnO, after treatment led to a clear decrease in *Staphylococcus aureus* total cell counts.

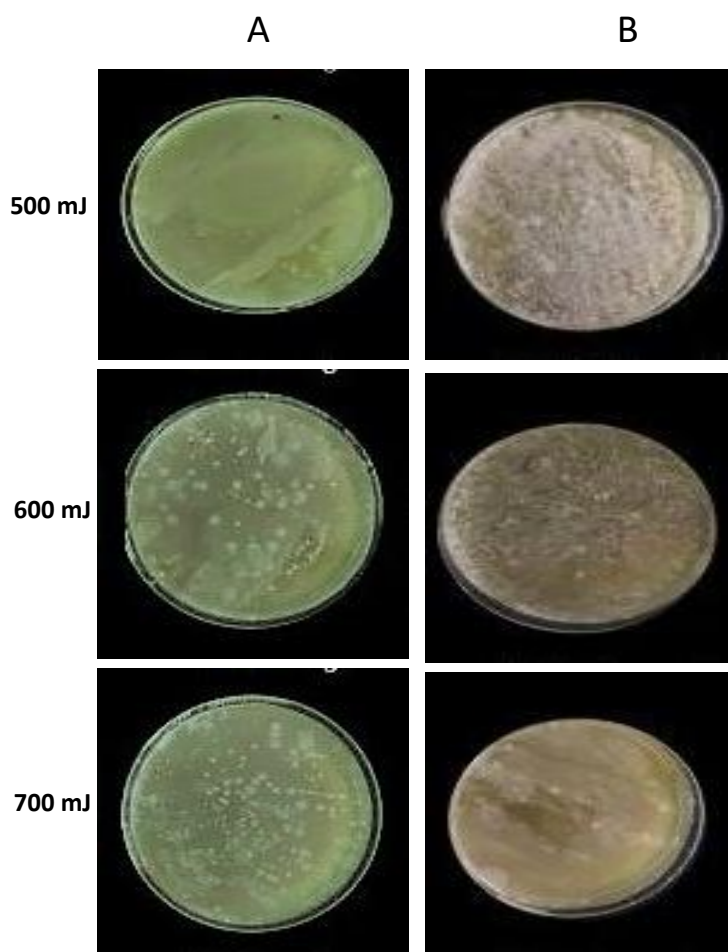


**Fig. 8:** *Staphylococcus* bacteria samples A: before being handling with nanoparticles of changed energy B: afterward handling through nanoparticles at different laser energies.

We note from the results of the [Table \(4\)](#) that increasing the laser energy from 500, 600 and 700 m J for ZnO, after treatment led to a clear decrease in *Staphylococcus aureus* total cell counts.

**Table 4:** Total cell counts of *Staphylococcus* bacteria before and afterward handling through nanoparticles at different laser energies.

Laser Energy (mJ)	Total cell counts	
	Before Treatment	after Treatment
500	$5 \times 10^9$	$0.9 \times 10^9$
600	$5 \times 10^9$	$0.8 \times 10^9$
700	$5 \times 10^9$	$0.7 \times 10^9$

#### 4. CONCLUSIONS

When ZnO nanoparticles prepared using the bombardment of pulse laser at a wavelength of (1064 nm) by pulsed laser ablation method in distilled water, they took a form of a hexagonal polycrystalline structure, at different energy levels of laser. The variation of energy level of laser

illustrates that the increasing laser energy cause increase in the crystalline size of ZnO, and decrease in the mean surface roughness, it observed that energy gap of Znic Oxide dropped due to increase of laser energy. Also, the ZnO experienced significant absorption at UV wavelength closed to visible light with different laser energy levels. In addition, by increasing laser energy aimed at ZnO after treatment led to a clear decrease in *Staphylococcus aureus*.

**Conflict of interests:** The author declared no conflicting interests.

**Sources of funding:** This research did not receive any specific grant from funding agencies in the public, commercial, or not-for-profit sectors.

**Author contribution:** Author contributed in the study.

## REFERENCES

1. Jebur KH, Mohammed NJ. Dependence of the Structural and Optical Properties of Gallium Oxide Nanostructures on Laser Fluency. *Al-Mustansiriyah Journal of Science*. 2021;32(4):60-6. <https://doi.org/10.1016/j.rineng.2022.100646>
2. Balachandran A, Sreenilayam SP, Madanan K, Thomas S, Brabazon D. Nanoparticle production via laser ablation synthesis in solution method and printed electronic application-A brief review. *Results in Engineering*. 2022; 16:100646. <https://doi.org/10.1016/j.rineng.2022.100646>
3. Fouad H, Yang G, El-Sayed AA, Mao G, Khalafallah D, Saad M, et al. Green synthesis of AgNP–ligand complexes and their toxicological effects on *Nilaparvata lugens*. *Journal of nanobiotechnology*. 2021;19:1-17. <https://doi.org/10.1186/s12951-021-01068-z>
4. Willander M, Nur O. Nanobiology and nanomedical devices using zinc oxide nanostructures. *Zinc Oxide Nanostructures: Advances and Applications*. 2014:127.
5. Jaber GS, Khashan KS, Abbas MJ, editors. Study the characteristics optical and structure properties of ZnO-nanoparticles fabricated by laser ablation in liquid. *Journal of Physics: Conference Series*; 2021: IOP Publishing. <https://iopscience.iop.org/article/10.1088/1742-6596/1795/1/012004>
6. Bhunia AK. ZnO nanoparticles: Recent biomedical applications and interaction with proteins. *Curr Trends Biomed Eng Biosci*. 2017;6(1). <http://dx.doi.org/10.19080/CTBEB.2017.06.555676>
7. Rashid TM, Nayef UM, Jabir MS, Mutlak FA-H. Synthesis and characterization of Au: ZnO (core: shell) nanoparticles via laser ablation. *Optik*. 2021;244:167569. <https://doi.org/10.1016/j.ijleo.2021.167569>
8. Radičić R, Maletić D, Blažeka D, Car J, Krstulović N. Synthesis of silver, gold, and platinum doped zinc oxide nanoparticles by pulsed laser ablation in water. *Nanomaterials*. 2022;12(19):3484. <https://doi.org/10.3390/nano12193484>
9. Ahmed BS, Mohammad SJ, Mohammed GH. The Effect of Laser Energy on the Structural, Optical and Electrical Properties of CdO Nanomaterials Generated Using (PLD) Technology, and Fabrication a Gas Sensor. *Tikrit Journal of Pure Science*. 2024;29(1):107-18. <https://doi.org/10.25130/tjps.v29i1.1451>
10. Faisal S, Jan H, Shah SA, Shah S, Khan A, Akbar MT, et al. Green synthesis of zinc oxide (ZnO) nanoparticles using aqueous fruit extracts of *Myristica fragrans*: their characterizations and biological and environmental applications. *ACS omega*. 2021;6(14):9709-22. <https://doi.org/10.1021/acsomega.1c00310?rel=cite-as&ref=PDF&jav=VoR>
11. Mandal AK, Katuwal S, Tettey F, Gupta A, Bhattarai S, Jaisi S, et al. Current research on zinc oxide nanoparticles: synthesis, characterization, and biomedical applications. *Nanomaterials*. 2022;12(17):3066. <https://doi.org/10.3390/nano12173066>
12. Mohammed NJ, Dagher HF. Synthesis and characterization of mercuric sulfide nanoparticles thin films by Pulsed Laser Ablation (PLA) in Distilled Water (DW). *Thin Films Laboratory, College of Science, Mustansiriyah University, Baghdad, Iraq*. 2020. <http://dx.doi.org/10.22068/ijmse.17.3.11>
13. Srikanth C, Madhu GM, Bhamidipati H, Srinivas S. The effect of CdO–ZnO nanoparticles addition on structural, electrical and mechanical properties of PVA films. *AIMS Materials Science*. 2019;6(6):1107-23. <https://doi.org/10.3934/matersci.2019.6.1107>
14. Omar ST, Ali WK, Karim AS. The Effects of Zinc Oxide nanoparticles synthesized from Eucalyptus plant extracts against mealworm stages *Tenebrio molitor* L., 1758 (*Tenebrionidae*: *Coleopetera*). *Tikrit Journal of Pure Science*.

2023;28(6):11-24.

<https://doi.org/10.25130/tjps.v28i6.1374>

15. Abdelghani GM, Ahmed AB, Al-Zubaidi AB. Synthesis, characterization, and the influence of energy of irradiation on optical properties of ZnO nanostructures. *Scientific Reports*. 2022;12(1):20016. <https://doi.org/10.1038/s41598-022-24648-x>

16. Aldwayyan A, Al-Jekhedab F, Al-Noaimi M, Hammouti B, Hadda T, Suleiman M, et al. Synthesis and characterization of CdO nanoparticles starting from organometallic dmphen-CdI<sub>2</sub> complex. *International Journal of Electrochemical Science*. 2013;8(8):10506-14. [https://doi.org/10.1016/S1452-3981\(23\)13126-9](https://doi.org/10.1016/S1452-3981(23)13126-9)

17. Abdulrahman NBA, Nssaif ZM. Antimicrobial activity of zinc oxide, titanium dioxide and silver nanoparticles against methicillin-resistant *Staphylococcus aureus* Isolates. *Tikrit*

*Journal of Pure Science*. 2016;21(3):49-53.

<https://doi.org/10.25130/tjps.v21i3.995>

18. Mendes CR, Dilari G, Forsan CF, Sapata VdMR, Lopes PRM, de Moraes PB, et al. Antibacterial action and target mechanisms of zinc oxide nanoparticles against bacterial pathogens. *Scientific reports*. 2022;12(1):2658. <https://doi.org/10.1038/s41598-022-06657-y>

19. Al-Fakeh MS, Alsaedi RO, Amiri N, Allazzam GA. Synthesis, characterization, and antimicrobial of MnO and CdO nanoparticles by using a calcination method. *Coatings*. 2022;12(2):215.

<https://doi.org/10.3390/coatings12020215>

20. C. Naik M, H. Kini J, BE KS, Velho-Pereira S. Sensor and antibacterial research of *Mussaenda frondosa* leaf extract assisted zinc oxide nanoparticles. *Sensing Technology*. 2024;2(1):2385839.

<https://doi.org/10.1080/28361466.2024.2385839>